Central Coulomb effects on pion interferometry

D. Hardtke and T. J. Humanic
Department of Physics, The Ohio State University, Columbus, Ohio 43210
(Received 2 October 1997)

Using a simple final-state rescattering model coupled with a simple Coulomb model, the effects of the central Coulomb potential on pion interferometry measurements in 158 GeV/nucleon Pb+Pb collisions are explored. Although the central Coulomb potential does not introduce correlations between pions, it does prevent an accurate measurement of the momentum difference. This momentum difference smearing effect leads to a reduction in the measured correlation radii and lambda parameters. These distortions are important in 158 GeV/nucleon Pb+Pb collisions because of large source sizes and the strong central Coulomb potential. [S0556-2813(98)04306-4]

PACS number(s): 25.75.Gz

I. INTRODUCTION

Pion interferometry is a useful tool for probing the freeze-out conditions in relativistic heavy-ion collisions, but in order to interpret the measured correlation radii it is very important to understand any final-state interactions that may distort the measurements. Recent NA44 measurements of the transverse mass ($m_T=\sqrt{p_T^2+m^2}$) dependence of the π^-/π^+ ratio in 158 GeV/nucleon Pb+Pb collisions [1] show a noticeable enhancement in the π^-/π^+ ratio at low m_T. This enhancement has been interpreted as evidence for a strong Coulomb interaction between the pion emitting source and the outgoing pions [1,2]. The strong central Coulomb potential is created by the primary protons in the projectile and target nuclei.

This work explores the influence of this central Coulomb potential on two-pion Bose-Einstein correlation measurements. The single particle data [1] suggest that central Coulomb effects will be important only for low-p_T pion correlation measurements, but these measurements have been shown to be most sensitive to the lifetime of the pion emitting source [3]. It is thus important to understand the central Coulomb effects in order to extract useful information from pion interferometry measurements. Although the Au+Au system at 10.8 GeV/c is not studied explicitly in this work, the qualitative conclusions should be applicable at these energies since a similar enhancement in the π^-/π^+ ratio is seen at these energies [4,5].

II. RESCATTERING+COULOMB MODEL

As input to these calculations, 158 GeV/nucleon Pb+Pb events from a simple rescattering model were used. A brief summary of the rescattering calculation used is given below. More information about this method can be found elsewhere [6–8]. Rescattering is simulated using a Monte Carlo cascade calculation which assumes strong binary collisions between hadrons. In addition to the more common hadrons such as pions, kaons, and nucleons, the calculation also includes the ρ, ω, η, η', ϕ, Δ, and K^* resonances. Resonances can be present at hadronization and also can be produced as a result of rescattering. Relativistic kinematics is used throughout. Isospin-averaged scattering cross sections are taken from Prakash *et al.* [9].

The Hanbury-Brown–Twiss (HBT) source sizes extracted from this model are in reasonable agreement with the measured source sizes form S+Pb and S+Ag collisions at 200 GeV/nucleon and preliminary Pb+Pb data at 158 GeV/nucleon [7,8]. The rescattering process generates strong position-momentum correlations, leading to a p_T dependence of the extracted radius parameters that matches the experimental observations for the S-induced collisions. The position-momentum correlations produced in the rescattering stage are important for the Coulomb calculations.

This model uses isospin averaged cross sections. Thus, for example, all π^0, π^+, and π^-'s are treated as generic π's during the rescattering stage. Coulomb interactions are assumed to not be important during the strong rescattering stage. The effects of the Coulomb interaction are added after freeze-out using an analytic correction to the particle momenta.

The model produces a list of particle freeze-out positions and momenta. Coulomb interactions are added by assuming that these particles are produced in a classical Coulomb potential [10]. The average classical Coulomb potential is

$$V_s=\frac{Z_{\rm eff}\,e^2}{r_a}, \tag{1}$$

where $Z_{\rm eff}$ is the effective charge and r_a is the average freeze-out radius. Of course, in a realistic model, each particle is produced in a different Coulomb potential that depends on freeze-out time and position. Using the average Coulomb potential, however, is computationally much simpler and should not change the qualitative conclusions.

Using simple energy and momentum conservation, the momentum of the particle at freeze-out can be related to the momentum of the particle at the detector using

$$E(p)=E(p_i)+V_s, \tag{2}$$

where p is the measured momentum of the particle, p_i is the momentum of the particle at freeze-out, $E(p)=(p^2+m^2)^{1/2}$, and V_s is the effective average Coulomb potential.

 © 1998 The American Physical Society

Note that V_s is positive for positive particles and negative for negative particles. Using this equation, the momentum shift for each particle is calculated:

$$\Delta p = p - p_i . \tag{3}$$

Up to this point the calculation is identical to Ref. [10]. In Refs. [10,11], the π^+/π^- ratio at midrapidity is calculated to be

$$\frac{N(\pi^+)}{N(\pi^-)} \propto \frac{\sqrt{p_t^2 - 2E(p_t)|V_s| + V_s^2}[E(p_t) - |V_s|]}{\sqrt{p_t^2 + 2E(p_t)|V_s| + V_s^2}[E(p_t) + |V_s|]}. \tag{4}$$

This expression has several assumptions. It assumes that any difference between the shapes of the charged pion spectra and neutral pion spectra is due entirely to Coulomb interactions. In addition, it assumes that the neutral pion spectra slope is constant as a function of transverse mass. There is an additional momentum shift term $N_0(E-V_s)/N_0(E+V_s)$, but for the nearly exponential pion spectra predicted by the rescattering model this term is constant as a function of transverse mass and only contibutes to the normalization of the ratio. Even if this momentum shift term is not strictly constant as a function of transverse mass, it was pointed out in Ref. [12] that for particles at low momentum in the fireball rest frame the Coulomb phase-space factor, from which Eq. (4) was derived, will dominate.

The effect of the central Coulomb potential on the measured momentum difference is calculated to be [10]

$$Q \approx Q_i \left(1 + \frac{V_s}{p_i} \right), \tag{5}$$

where Q_i is the momentum difference at freeze-out and Q is the measured momentum difference. This formula predicts that negatively charged particle pairs will give a measured source size that is larger than the actual source size and that positively charged pairs will give a measured source size that is smaller than the actual source size.

The simple analytical calculation [10] does not include any directional dependence. Correlation functions are typically measured experimentally in three dimensions and parametrized by [13]

$$C_2(\vec{Q},\vec{k}) = 1 + \lambda \ \exp[-R_{t_o}^2(\vec{k})Q_{t_o}^2 - R_{t_s}^2(\vec{k})Q_{t_s}^2 - R_l^2(\vec{k})Q_l^2], \tag{6}$$

where $\vec{k} = \vec{p}_1 + \vec{p}_2$ is the total momentum of the pair, Q_l is the momentum difference in the beam direction, Q_{t_o} is the momentum difference in the direction transverse to beam and parallel to the total transverse momentum of the pair, and Q_{t_s} is the momentum difference in the direction transverse to beam and perpendicular to the total transverse momentum of the pair. In this work, the directional dependence is explicitly considered. Δp is calculated analytically using Eq. (3), and then the directional dependence is added using

$$\vec{p} = \vec{p}_i + \Delta p \hat{x}, \tag{7}$$

where $\hat{x}$ is the unit vector in the direction of the freeze-out position $\vec{x}$. Because of the very strong position-momentum correlations generated by the final-state rescattering $\hat{x} \cdot \hat{p} \simeq 1$. This allows us to approximate the problem using Eqs. (3) and (7) but it should be noted that this simple prescription would fail for models without strong position-momentum correlations. This approach also assumes that the central Coulomb charge is spherically symmetric.

The procedure used in these calculations is the following. Events were generated using the simple rescattering model. This produces a list of pion freeze-out momenta and positions. The Coulomb potential is added using Eqs. (2), (3), and (7). The correlation functions are then calculated using the procedure described in Refs. [6,7]. All correlation functions are evaluated in the longitudinally comoving system (LCMS) frame where $p_{z_1} + p_{z_2} = 0$. The only free parameter in the calculation is magnitude of the average Coulomb potential V_s.

III. RESULTS AND DISCUSSION

The average Coulomb potential V_s is found by fitting Eq. (4) to the NA44 data [1]. The NA44 data is not absolutely normalized, so the overall normalization is left as a free parameter in the fit. The value of V_s extracted from the single particle data is ≈ 5 MeV. This is actually a lower limit on the Coulomb potential since Eq. (4) is the midrapidity limit ($y = 2.9$) and the NA44 data was measured over the rapidity range $3.1 < y < 4.1$. This value of V_s is still large enough to have effects on the measured pion correlation functions.

In order to facilitate comparison to future experimental data, the pion correlation functions are calculated for the low p_T NA44 acceptance [13]. The rapidity and p_T range are $0 < p_T < 400$ MeV/c and $3.1 < y < 4.1$, respectively, and the mean p_T is approximately 150 MeV/c. The correlation function is calculated with three values of V_s: $V_s = 0$ (i.e., no Coulomb effects), $V_s = 5$ MeV (i.e., $\pi^+\pi^+$), and $V_s = -5$ MeV (i.e., $\pi^-\pi^-$).

Figure 1 compares the momentum difference shifts in Q_{t_s}, Q_{t_o}, and Q_l for the positive pion pairs ($V_s = 5$ MeV) and the negative pion pairs ($V_s = -5$ MeV). These momentum difference shifts are then characterized by a mean momentum difference shift and an rms deviation of the momentum difference shift, and the values are listed in Table I. In addition, Table I lists the mean momentum difference shift and rms deviation of this shift for low $\vec{Q}$ pairs ($|Q_{t_s}|, |Q_{t_o}|, |Q_l| \leq 50$ MeV/c). Figure 1 and Table I show that the mean shift in all three components of the momentum difference is small. If only low $\vec{Q}$ pairs are considered, the momentum difference shift becomes negligable. This is what would be expected since pions of similar momentum should experience roughly the same Coulomb impulse. The rms deviations of the momentum shift, however, are significantly larger than the mean shifts. Although the net momentum difference shift is small, the direction of the momentum difference vector is changed appreciably by the central Coulomb potential.

The projections of the correlation functions in the NA44 acceptance with and without the central Coulomb potential are shown in Fig. 2, and the extracted fit parameters are listed in Table II. The extracted radii are smaller for both the positive and negative Coulomb potentials compared to the extracted radii without the Coulomb potential, and the reduc-

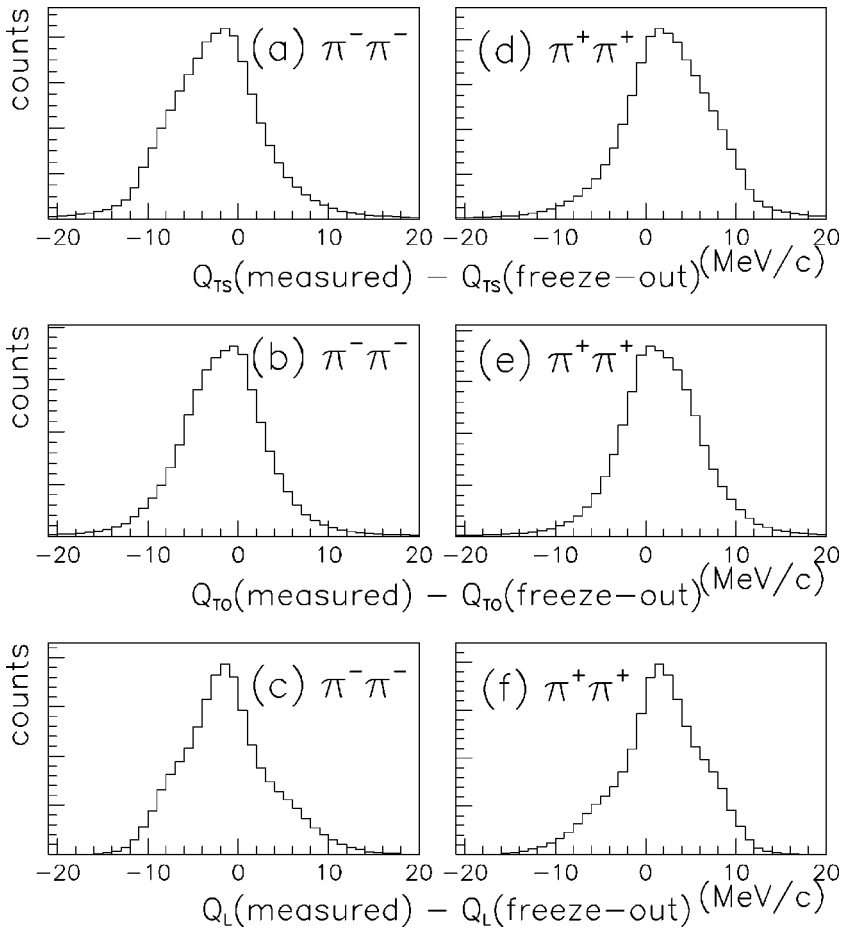

FIG. 1. The shifts in Q_{t_s},Q_{t_o}, and Q_l due to the central Coulomb potential for negative (a)–(c) and positive (d)–(f) pion pairs. The average Coulomb potential $V_s = 5$ MeV.

tion is largest for R_l. The magnitude of the reduction in R_l and λ is largest for the negative pions. The transverse radius parameters (R_{t_s} and R_{t_o}) are affected only slightly.

There are two effects due to the central Coulomb potential that lead to a distortion of the correlation function. The central Coulomb potential introduces a net shift in the momentum difference. This net shift was pointed out in Refs. [10,14]. The net shift in the momentum difference, however, has only a small effect compared to the momentum difference smearing effect. The momentum difference smearing effect, characterized by the rms of the momentum difference shift distributions, is the more important of the two effects and leads to a reduction of the measured radii and lambda parameters. The effect is similar to the well understood effect of the experimental momentum resolution on the correlation function. The momentum difference smearing due to the central Coulomb potential is similar for Q_{t_s},Q_{t_o}, and Q_l, but, due to the larger radius in the longitudinal direction, the change in the extracted radius is largest for R_l.

In Ref. [10] only the net momentum difference shifts were considered. This leads to the conclusion that positively charged pairs should measure a source size smaller than the true source size and negatively charged pairs should measure a source size larger than the true source size. A more sophisticated approach was taken in Ref. [14], and the results were qualitatively similar. The present results are qualitatively dif-

TABLE I. The mean and rms deviations of the momentum difference shifts caused by the central Coulomb potential for negative and positive pion pairs.

	$\pi^-\pi^-$		$\pi^+\pi^+$	
	mean (MeV/c)	rms (MeV/c)	mean (MeV/c)	rms (MeV/c)
ΔQ_{t_s} (all $\vec{Q}$)	−2.4	6.4	2.5	6.3
ΔQ_{t_o} (all $\vec{Q}$)	−1.6	6.0	1.7	5.9
ΔQ_l (all $\vec{Q}$)	−1.3	5.0	1.5	4.8
ΔQ_{t_s} ($\lvert Q_{t_s}\rvert$,$\lvert Q_{t_o}\rvert$,$\lvert Q_l\rvert \leq 50$ MeV/c)	−0.2	3.6	0.5	3.6
ΔQ_{t_o} ($\lvert Q_{t_s}\rvert$,$\lvert Q_{t_o}\rvert$,$\lvert Q_l\rvert \leq 50$ MeV/c)	−0.2	3.5	0.4	3.4
ΔQ_l ($\lvert Q_{t_s}\rvert$,$\lvert Q_{t_o}\rvert$,$\lvert Q_l\rvert \leq 50$ MeV/c)	−0.1	4.9	1.0	4.8

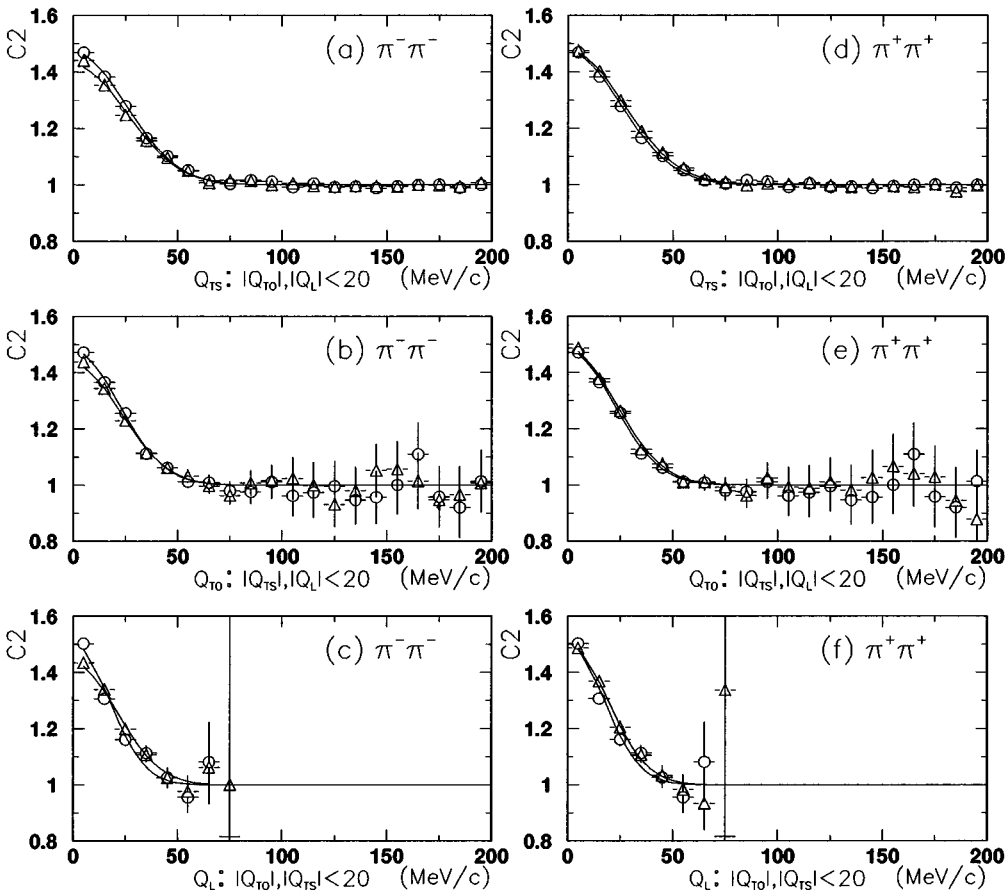

FIG. 2. The projections of the correlation functions (C2) in Q_{t_s},Q_{t_o}, and Q_l for positive and negative pions (open triangles) compared with the projections without the central Coulomb potential (open circles). The fit functions are also included. The projections are over the lowest 20 MeV in the other momentum difference directions.

ferent than both Refs. [10,14] in that both negative and positive pairs measure a source size smaller than the true source size.

There are several possible reasons for the discrepancy with Ref. [14]. First, a static, spherical source is used in Ref. [14], whereas we use a dynamical source with position-momentum correlations. An expanding source leads to a $Z_{\rm eff}$ that is much less that the true nuclear charge [2,15,16]. The source used here ($R_g \approx 6-7$ fm) is larger than the source used in Ref. [14] ($R_g = 4.5$ fm), and a larger source increases the importance of the momentum difference smearing. In addition, the method of extracting the radius parameters in the present work is also different than Ref. [14]. Here, the three-dimensional correlation function is fit using Eq. (6). In Ref. [14], the fit is only performed in the transverse directions, and the intercept parameter is assumed to be unity. Even without resonances, momentum difference smearing can lead to intercept parameters reduced from unity. Hence, it must be included in the fit function.

TABLE II. The fitted results of the gaussian parametrization of the correlation functions for pions without the central Coulomb potential, with a negative Coulomb potential ($\pi^-\pi^-$), and with a positive Coulomb potential ($\pi^+\pi^+$).

V_s(MeV)	R_{t_s}(fm)	R_{t_o} (fm)	R_l (fm)	λ
0.0	5.55±0.12	6.37±0.26	8.13±0.63	0.63±0.03
−5.0 ($\pi^-\pi^-$)	5.53±0.09	6.17±0.06	6.73±0.13	0.54±0.01
5.0 ($\pi^+\pi^+$)	5.33±0.10	6.14±0.16	7.38±0.22	0.62±0.02

The problem of the central Coulomb potential on the measured pion correlation functions was also addressed in Ar +KCl collisions at 1.8 GeV/nucleon [17]. The approach used, however, was much different than that used here. In Ref. [17], an attempt was made to correct the experimental data for the central Coulomb distortions. The momentum shift of each pion due to the central Coulomb charge was calculated using a formalism correct in both the classical and quantum mechanical limit [12]. It was found that the central Coulomb effect on the measured correlation function was small compared to the experimental error on the measured radii. The measured radii in Ref. [17] were much smaller than the predicted radii in Pb+Pb collisions at 158 GeV/nucleon, so the momentum difference smearing effect should be much less important.

IV. CONCLUSIONS

Using a simple rescattering model and a classical Coulomb model, it was shown that the central Coulomb potential

in 158 GeV/nucleon Pb+Pb collisions causes a reduction in the measured HBT radii and lambda parameters for charged pions. This effect should be considered when comparing theoretical predictions to experimental data.

ACKNOWLEDGMENTS

We wish to thank Michael Lisa and Nu Xu for useful discussions. This work was supported by NSF Grant No. PHY-9511850.

[1] H. Bøggild *et al.*, Phys. Lett. B **372**, 339 (1996).
[2] H. W. Barz, J. P. Bondorf, J. J. Gaardhøje, and H. Heiselberg, Phys. Rev. C **56**, 1553 (1997).
[3] D. E. Fields, J. P. Sullivan, J. Simon-Gillo, H. van Hecke, B. V. Jacak, and N. Xu, Phys. Rev. C **52**, 986 (1995).
[4] L. Ahle *et al.*, Nucl. Phys. **A610**, 139c (1996).
[5] J. Barrette *et al.*, Nucl. Phys. **A610**, 153c (1996).
[6] T. J. Humanic, Phys. Rev. C **50**, 2525 (1994).
[7] T. J. Humanic, Phys. Rev. C **53**, 901 (1996).
[8] T. J. Humanic, Phys. Rev. C **57**, 866 (1998).
[9] M. Prakash, M. Prakash, R. Venugopalan, and G. Welke, Phys. Rep. **227**, 321 (1993).
[10] G. Baym and P. Braun-Munzinger, Nucl. Phys. **A610**, 286c (1996).
[11] P. Braun-Munzinger (private communication).
[12] M. Gyulassy and S. K. Kaufmann, Nucl. Phys. **A362**, 503 (1979).
[13] H. Bøggild *et al.*, Phys. Lett. B **349**, 386 (1995).
[14] H. W. Barz, Phys. Rev. C **53**, 2536 (1996).
[15] T. Osada, S. Sano, M. Biyafima, and G. Wilk, Phys. Rev. C **54**, R2167 (1996).
[16] A. Ayala and J. Kapusta, Phys. Rev. C **56**, 407 (1997).
[17] W. A. Zajc *et al.*, Phys. Rev. C **29**, 2173 (1984).